FUDMA Journal of Sciences (FJS)
ISSN online: 2616-1370
ISSN print: 2645 - 2944
Vol. 10 No. 17, September, 2026, pp 74 – 85
DOI: https://doi.org/10.33003/fjs-2026-1017-5885

The Effects of Soret on Steady State Magnetohydrodynamic Heat Transfer Flow of Jeffrey Nanofluid with Nonlinear Thermal Radiation

***[1]Williams Michael, [1]Akeem Babatunde Disu, [1]Christie Yemisi Ishola, [2]Yakubu Bello, [3]Zainab Abubakar Dogondaji and [1]Ayuba Adams**

[1]Department of Mathematics, National Open University of Nigeria.
[2]Department of Mathematics and Statistics, Air Force Institute of Technology, Kaduna, Nigeria.
[3]Department of Mathematics, Sokoto State University, Sokoto, Nigeria.

*Corresponding authors' email: michealwilliams185@gmail.com

Received: 04 Aug. 2026
Accepted: 12 Aug. 2026
Published: 21 Sept. 2026

ABSTRACT
The study investigated how thermo diffusion alters fluid properties, the heat absorption capacity of permeable media, the stability of MHD heat transfer in Jeffrey nanofluid under convective boundary conditions, and key dimensionless factors governing the flow. The mathematical model was initially transformed into ordinary differential equations via Lie symmetry group renovation. These renovated equations were then numerically solved using a bvp4c MATLAB solver, with outcomes presented through graphs and tables. Model validation against the published results demonstrated excellent agreement, with a maximum relative discrepancy of approximately 0.00021% in the reduced skin-friction values. The porosity, magnetic and Jeffrey parameters notably diminishes the velocity of Jeffrey nanofluid. Significant enhancements in temperature flow were observed with the inclusion of nonlinear thermal radiation, heat source-sink parameters, and the Biot number. Additionally, the Soret parameter positively influences mass transfer, while the Lewis number and chemical reaction parameters act as stabilizing factors. Considering the unique properties of Jeffrey fluids in conjunction with nanomaterials, the findings of this study are anticipated to hold practical significance in industries such as polymer, metallurgy, chemicals, and automobiles.

Keywords: Porous Material, Thermophoresis, Thermodiffusion, Nonlinear Thermal Radiation, Heat Source-Sink

INTRODUCTION

The impact of Soret has been adopted by countless researchers in their work, which is crucial from an engineering standpoint for the storage of petroleum reservoirs, nuclear waste, and other materials. Soret's effect is the temperature slope, which is caused by mass fluxes that are located in the mass equation. Irfan and Muhammad (2023) looked at the computational framework of MHD radiative heat transfer to carreau nanofluid with Soret-Dufour effects and activation energy. The impact of thermo-diffusion and diffusion-thermo on magnetohydrodynamic heat and mass transmission in a tube was discussed by Khan et al. (2017). It was observed that by enhancing diffusion-thermo and thermo-diffusion, mass and heat transmission are progressive. Using an extended sheet, Bidemi and Ahamed (2019) also with Williams and Yabo (2024) examined magnetohydrodynamic nanoliquids, addressing both diffusion-thermo and thermo-diffusion aspects of their research. Diffusion-thermo decreased the mass transfer, while thermo-diffusion developed the heat transfer. These studies demonstrate that Soret mechanisms can substantially modify the coupled thermal and concentration fields. However, most existing investigations have considered these effects in relatively different fluid models and geometries, with limited attention to their combined interaction with Jeffrey fluid behaviour, porous-medium resistance, and nonlinear thermal radiation. This provides motivation for incorporating cross-diffusion effects into a more comprehensive non-Newtonian MHD flow model.

A nanofluid is a based fluid that contains dense, minute particles. Examples of nanofluids include ethanol fuel, oil, water, glycol, and so on. Nanofluids can also be thought of as a method of amplifying the effect of heat transfer in liquids. Car engines and welding equipment can be treated with nanofluid to lower the temperature of high heat flux devices, like high microwave tubes. Transportation, nuclear reactors, home refrigerator engines, biomedicine, food storage, fuel cells, and microelectronics are just a few of the industries that can benefit from nanofluid. The Sutterby nanofluid flow under shear thickening and shear thinning behaviour over biaxially stretchable exponential and nonlinear sheets was examined by Ishtiaq et al. (2023) for variable physical effects. The impact of heat source-induced thermal slip-on trihybrid nanofluid flow across an extended surface was investigated by Ali et al. in 2023. Three distinct shaped nanoparticles were used by Hasnain et al. (2023) to assess thermal growth in ternary nanofluids based on motor oil and water over linear and nonlinear stretching sheets. Powell nanoliquid with the appearance of viscosity was found in an upright partition by Lawal et al. in 2022. By using thermophoresis and advancing Brownian motion, the temperature outline accelerates and takes the inverse case for fluid concentration. Analytical work was done by Aman et al. (2017) to thin out the Casson liquid stream of different convective heat transfer of multiwall and single-wall carbon nanotubes on a perpendicular sheet. Interval fractional offshoots were examined by Aman et al. (2018) using convective magnetohydrodynamic nanofluid flow in an expanding surface. Recycled nanofluid can be used in manufacturing facilities to create solar energy resources. In a parallel plate, Abbas et al. (2020) investigated the Rosseland approximation for heat radiation and leaky nanoliquid surfaces. Sobamowo (2018) examined how nanoparticles along an expanding sheet are affected by magnetohydrodynamics. Brownian motion and thermophoresis were included in the magnetohydrodynamic heat transfer flow of nanoliquid along a parallel plate that was conducted by Das et al. (2017). Recently, Disu et al (2026) reported on MHD hybrid nanofluid in a vertical channel with engine oil as the base fluid under Poiseuille and Couette flow Collectively, these investigations establish the importance of non-Newtonian behaviour, nanoparticle transport, Brownian motion, thermophoresis, and thermal radiation in controlling heat and mass transfer. Nevertheless, the existing Jeffrey nanofluid literature has generally treated these mechanisms separately or in limited combinations. In particular, the simultaneous effects of Soret diffusion, porous resistance, nonlinear thermal radiation, magnetic forces, and Jeffrey fluid parameters remain insufficiently explored.

Nonetheless, a conventional method for obtaining correspondence reduction of nonlinear differential equation is the Lie group technique. Partial differential equations can be converted to ordinary differential equations with fewer variables by applying the similarity transformation. Scaling group conversion, a unique type of Lie group analysis that is frequently employed in nonlinear dynamical structures, is set up to create similarity transformations. Numerous scholars, such as Ahmad et al. (2022), Rashidi et al. (2014), and Kandasamy et al. (2011), use the Lie group.

Table 1: Nomenclature

Symbol	Description	Symbol	Description
Pr	Prandtl number	M	Magnetic parameter
Ra	Rayleigh number	Le	Lewis number
Nr	Buoyancy ratio	Nb	Brownian motion parameter
Nt	Thermophoresis parameter	N	Thermal radiation parameter
B_0	Magnetic field strength	ρ_f	Density of base fluid
u, v	Velocity components along x, y-axis	T	Temperature variable
$(\rho c)_p$	Nanoparticles specific heat	C_∞	Ambient liquid concentration
τ	Heat capacity ratio	σ_1	Stefan-Boltzmann constant
C	Nanoparticles concentration	Q_0	Non-uniform heat generation
K^*	Mean absorption coefficient	k_1	Absorption coefficient
T_∞	Ambient liquid temperature	Q	Heat source/sink
$(\rho c)_f$	Fluid specific heat	Bi	Biot number
β	Deborah number	Ct	Temperature ratio
S	Mass transfer parameter	κ	Thermal conductivity
D_B	Brownian diffusion	D_T	Termophretic diffusion
C_1	Specific heat at constant pressure	K	Porous material
U	Free stream velocity of the flow	C_w	Reference concenteration
T_w	Reference temperature	g	Gravitational acceleration
f	Dimensionless velocity	Sr	Soret parameter
$U(x)$	Velocity of the exterior stream	$B(x)$	Transverse magnetic field
v_∞	Condition far away from the plate	b	Constant
γ	Chemical reaction parameter	σ	Electrical conductivity
ν	Kinematic viscosity	λ	Jeffrey parameter
λ_1	Relaxation time	η	Similarity variable
ψ	Stream function	θ	Dimensionless temperature
ϕ	Dimensionless concentration	α	Thermal diffusivity
ω	Volumetric thermal expansion coefficient of the base fluid		

The researchers working in fluid technicality have been informed of a completely new trend by the invention of Jeffrey nanofluid. Muhammad et al. (2021) Jeffrey nanofluid heat transfer using reflected magnetohydrodynamics using parallel plates. Thermophoresis was employed to demonstrate the identification of nanofluid Brownian motion. Convective conditions of the magnetohydrodynamic Jeffrey nanoliquid on a perpendicular plate were presented by Hayat et al. (2017). In an upright plate, Reddy and Makinde (2016) examined the MHD flow of Jeffrey nanofluid. They converted the system of partial differential equations into an ordinary differential equation system by making wavelength assumptions. In a perpendicular channel, Waqas et al. (2019) reported linear thermal radiation using an external heat source-sink of Jeffrey nanofluid. The MHD Jeffrey nanoliquid was strengthened by Abbasi et al. (2016) using thermophoresis and Brownian motion in the flow.

Because porous materials are used in nuclear reactors, automobile industries, food processing and storage, fibre insulation, and other fields, they have drawn a lot of attention from researchers throughout the years. The Dufore effect across a parallel plate and Jeffrey nanofluid with porous material were studied by Michael and Isah (2023). The artificial neural network method was created by Nasir et al. (2023) to forecast the thermal transport study of nanofluid inside a porous enclosure. The fluid's velocity was positively impacted by the porous material's action. Rana (2021) discussed the Darcy model for a porous media using Jeffrey nanofluid as the basis fluid in a convective Jeffrey nanofluid flow. Zin et al. (2017) investigated magnetohydrodynamics (MHD) with thermal radiation and a porous media. Convective heating conditions on the flow of Jeffrey nanofluids with coupled porous and magnetic effects were demonstrated by Khan and Shehzad (2020). These studies confirm that porous resistance can significantly alter momentum and thermal transport and that its interaction with magnetic and non-Newtonian effects is important in engineering flow systems. However, most existing porous-medium studies involving Jeffrey nanofluids do not simultaneously incorporate Soret diffusion, nonlinear thermal radiation, and internal heat generation or absorption. A more integrated treatment is therefore required to understand the coupled influence of these mechanisms on heat and mass transfer.

Furthermore, because of its potential use in engineering projects, nonlinear thermal radiation on a conducting heat and mass transfer on stretched sheets has garnered the interest of numerous researchers. In engineering operations where high temperatures are necessary for optimal performance, it is increasingly significant. Nonetheless, it is helpful in industrial processes like gas turbines, liquid metal fluid, power generation facilities, and others where the quality of the final output depends on heat regulation. In the presence of nonlinear thermal radiation, Bafakeeh et al. (2022) investigated the heat and mass transfer flow of nanofluid in an extended sheet with the result of porous medium and magnetic force. Electrically conducting viscous incompressible heat and mass transfer flow of mixed convection of nonlinear thermal radiation with suction/injection were hashed out by Jha and Samaila (2022). Other investigations on nonlinear thermal radiation include Isah et al. (2022), Abdullahi et al. (2022), Yabo et al (2023), Michael et al. (2023), Disu et al (2025), and Shuaibu et al (2026). The above studies demonstrate that nonlinear thermal radiation can substantially modify temperature distributions and heat-transfer rates, particularly when coupled with magnetic fields, porous resistance, and internal thermal effects. However, the combined influence of nonlinear thermal radiation with Jeffrey fluid behaviour and Soret effect remains relatively underdeveloped. This limitation is particularly important for vertical-channel configurations where buoyancy, magnetic forces, porous resistance, and coupled heat and mass transfer can interact simultaneously.

Although considerable progress has been made in the study of MHD nanofluid flow, heat and mass transfer, Soret effect, Jeffrey fluid behaviour, porous media, and nonlinear thermal radiation, the existing literature largely considers these physical mechanisms in isolation or in limited combinations. In particular, there remains a need for a comprehensive investigation that simultaneously accounts for Soret diffusion, nonlinear thermal radiation, porous-medium resistance, Jeffrey fluid characteristics, magnetic effects, and heat generation/absorption in buoyancy-driven flow through a vertical channel. The interaction of these mechanisms may significantly influence the velocity, temperature, and concentration distributions and, consequently, the skin-friction coefficient, Nusselt number, and Sherwood number.

Motivated by this gap, the present study investigates the combined effects of the Soret mechanism, nonlinear thermal radiation, porous-medium resistance, Jeffrey fluid characteristics, magnetic field, and heat generation/absorption on MHD buoyancy flow and heat and mass transfer in a vertical channel. Lie group analysis is employed to transform the governing partial differential equations into a system of ordinary differential equations through appropriate similarity transformations, while the resulting boundary-value problem is solved numerically using the MATLAB bvp4c solver. The study provides a comprehensive assessment of the influence of the governing parameters on the velocity, temperature, and concentration fields, as well as the skin-friction coefficient, Nusselt number, and Sherwood number. The results are expected to provide useful insights into the coupled transport mechanisms relevant to thermal management and other engineering applications involving electrically conducting non-Newtonian fluids.

MATERIALS AND METHODS

Flow Examination

Mathematical Formulation

Figure 1 present the flow geometry of two- dimensional free convective boundary layer flow of conducting Jeffrey nanofluid over a stretching sheet with nonlinear thermal radiation and porous material in the present of Soret effect. The flow is assumed to be in the *x*-direction which is taken along the plate and *y*-axis is normal to it with the non-uniform velocity $U(x)$and a uniform transverse magnetic of strength $B(x)=\frac{B_0}{\sqrt{x}}$ and $V(x)$ is the momentum of suction/injection, the energy wall is represented with T_w and the wall of concentration withC_w. Also in the flow, effect of thermophoresis and Brownian motion are taken into account. The magnetic Reynolds number of the flow is taken to be small enough so that induced magnetic field is assumed to be insignificant in contrast with applied magnetic field.

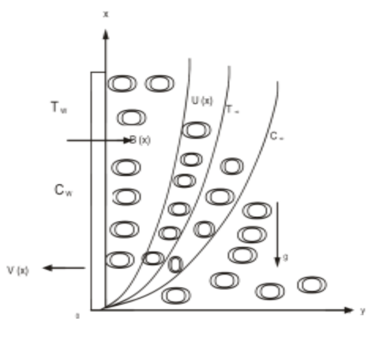

Figure 1: Geometry of the Flow for Porous Stretching Sheet

Applying the Boussinesq approximations we obtain the following governing equations as Ahmad *et al*. (2022)

$$\frac{\partial u}{\partial x}+\frac{\partial v}{\partial y}=0 \qquad (1)$$

$$u\frac{\partial u}{\partial x}+v\frac{\partial u}{\partial y}+\frac{\lambda_1 C_1}{1+\lambda}\left[u^2\frac{\partial^2 u}{\partial x^2}+v^2\frac{\partial^2 u}{\partial y^2}+2uv\frac{\partial^2 u}{\partial x\partial y}\right]=$$
$$=\frac{V}{1+\lambda}\frac{\partial^2 u}{\partial y^2}+\left[(1-C_\infty)\rho_{f_\infty}\omega(T-T_\infty)-(\rho_p-\rho_{f_\infty})(C-C_\infty)\right]g$$
$$-\frac{\sigma B^2(x)}{\rho_f}\left[u+\lambda_1 C_1 v u\frac{\partial u}{\partial y}\right]-\frac{v_\infty}{bk_1}u \qquad (2)$$

$$u\frac{\partial T}{\partial x}+v\frac{\partial T}{\partial y}=\frac{\kappa}{(\rho c)_f}\frac{\partial^2 T}{\partial y^2}-\frac{1}{(\rho c)_f}\frac{\partial q_r}{\partial y}+\frac{Q_0}{(\rho c)_f}(T-T_\infty)$$
$$+\tau\left[D_B\frac{\partial C}{\partial y}\frac{\partial T}{\partial y}+\frac{D_T}{T_\infty}\left(\frac{\partial T}{\partial y}\right)^2\right] \qquad (3)$$

$$u\frac{\partial C}{\partial x}+v\frac{\partial C}{\partial y}=D_B\frac{\partial^2 C}{\partial y^2}+\frac{D_T}{T_\infty}\frac{D_B k_1(T-T_\infty)}{T_w(C-C_\infty)}\frac{\partial^2 T}{\partial y^2}$$
$$-\frac{Uk}{D_B}(C-C_\infty) \qquad (4)$$

The boundary conditions for the above models are as follow:

$$\left.\begin{array}{l} u = U_w(x) = C_1 x v = v_w(x) \\ T = \frac{-k\partial T}{\partial y} hf(T_f - T) \\ C = C_w \end{array}\right\} at y = 0 \\ u \to 0, T \to T_{\infty,} C \to C_\infty as y \to \infty \quad (5)$$

Using Rosseland approximation, the radiative heat flux term q_r along $y$is expressed as follows

$$q_r = -\frac{4\sigma_1}{3k_1}\frac{\partial T^4}{\partial y} \quad (6)$$

In order to nonlinearized equation (6), expand T^4 about T_∞ into Taylor's series expansion gives

$$T^4 = (\theta(T_1 - T_0) + T_0)^4 \quad (7)$$

Substitute equation (6) and (7) into equation (3) we get

$$u\frac{\partial T}{\partial x} + v\frac{\partial T}{\partial y} = \left[1 + \frac{4N}{3}(Ct + \theta)^3\right]\frac{\partial^2 T}{\partial y^2} + \\ 4N[Ct + \theta]^2\left(\frac{\partial T}{\partial y}\right)^2 + \frac{Q}{(\rho c)_f}(T - T_\infty) \\ +\tau\left[D_B\frac{\partial C}{\partial y}\frac{\partial T}{\partial y} + \frac{D_T}{T_\infty}\left(\frac{\partial T}{\partial y}\right)^2\right] \quad (8)$$

Stream Function and Non- Dimensional Variables

Using stream functionψ, defined by

$$u = \frac{\partial\psi}{\partial y} and v = -\frac{\partial\psi}{\partial x} \text{ and } v = -\frac{\partial\psi}{\partial x} \quad (9)$$

together with non- dimensional variables illustrated below

$$\left.\begin{array}{l} \theta = \frac{T - T_\infty}{T_w - T_\infty}, \phi = \frac{C - C_\infty}{C_w - C_\infty}, \\ Pr = \frac{v}{\alpha}, M = \frac{\sigma B_0^2}{\rho_f}, \beta = \lambda_1 C_1, \\ Sc = \frac{D_B}{v}, K = \frac{v_\infty}{bk_1}, \\ Ra = \frac{(1 - \phi_\infty)\beta g \Delta\theta}{V}, \\ Le = \frac{\alpha}{D_B}, \gamma = \frac{Uk}{D_B}, y = \sqrt{\frac{C_1}{v}}y, \\ Q = \frac{Q_0}{(\rho c)_f}, \tau = \frac{(\rho c)_p}{(\rho c)_f}, x = \frac{C_1}{U_1}x, \\ Nb = \frac{D_B \Delta\phi(\rho c)_p}{\kappa}, u = \frac{u}{U_1}, \\ Nr = \frac{(\rho_p - \rho_{f\infty})\Delta\phi}{\rho_{f\infty}\beta\Delta\theta(1 - \phi_\infty)}, \\ N = \frac{4T_\infty^3\sigma_1}{K_1\kappa}, Nt = \frac{D_T\Delta\theta(\rho c)_p}{\kappa T_\infty},, \\ Sr = \frac{D_B k_1(T - T_\infty)}{T_w(C - C_\infty)}, \alpha = \frac{k}{(\rho c)_f} \end{array}\right\} \quad (10)$$

Equations (9) and (10) are substituted into equations **(**1), (2), (4), (5) and (8), note that equation (1) is satisfied identically. Hence the following are obtained

$$(1 + \lambda)\left[\frac{\partial\psi}{\partial y}\frac{\partial^2\psi}{\partial x\partial y} - \frac{\partial\psi}{\partial x}\frac{\partial^2\psi}{\partial y^2}\right] + \\ \beta\left[\left(\frac{\partial\psi}{\partial y}\right)^2\frac{\partial^3\psi}{\partial x^2\partial y} - \left(\frac{\partial\psi}{\partial x}\right)^2\frac{\partial^3\psi}{\partial y^3} - 2\frac{\partial\psi}{\partial y}\frac{\partial\psi}{\partial x}\frac{\partial^3\psi}{\partial x\partial y^2}\right] = \\ \frac{\partial^3\psi}{\partial y^3} + (1 + \lambda)Ra[\theta - N_r\phi] - \\ (1 + \lambda)M\left(\frac{\partial\psi}{\partial y} - \beta\frac{\partial\psi}{\partial x}\frac{\partial^2\psi}{\partial y^2}\right) - (1 + \lambda)\frac{1}{K}\frac{\partial\psi}{\partial y} \quad (11)$$

$$Pr\left[\frac{\partial\psi}{\partial y}\frac{\partial\theta}{\partial x} - \frac{\partial\psi}{\partial x}\frac{\partial\theta}{\partial y}\right] = \left[1 + \frac{4N}{3}(Ct + \theta)^3\right]\frac{\partial^2\theta}{\partial y^2} \\ +4N[Ct + \theta]^2\left(\frac{\partial\theta}{\partial y}\right)^2 + Q\theta + \\ N_b\frac{\partial\phi}{\partial y}\frac{\partial\theta}{\partial y} + N_t\left(\frac{\partial\theta}{\partial y}\right)^2 \quad (12)$$

$$Le\left[\frac{\partial\psi}{\partial y}\frac{\partial\phi}{\partial x} - \frac{\partial\psi}{\partial x}\frac{\partial\phi}{\partial y}\right] = \frac{\partial^2\phi}{\partial y^2} + \frac{N_t Sr}{N_b}\frac{\partial^2\theta}{\partial y^2} - \gamma\phi \quad (13)$$

The boundary condition becomes

$$\left.\begin{array}{l} \left.\begin{array}{l} \frac{\partial\psi}{\partial y} = x, -\frac{\partial\psi}{\partial x} = \frac{V_w}{\sqrt{C_1 v}}, \theta = \\ -B_i(1 - \theta), \phi = 1 \end{array}\right\} at y = 0 \\ \frac{\partial\psi}{\partial y} \to 0, \theta \to 0, \phi \to 0 \Big\} as y \to \infty \end{array}\right\} \quad (14)$$

Lie Group Exploration

Following the classical Lie group approach (Ahmad *et al* (2022) and Das *et al*. (2017)) the special scaling group transformations of equations (11) – (13) and (14) are defined by the following:

$$\left.\begin{array}{l} \Gamma: x^* = xe^{\varepsilon\alpha_1}, y^* = ye^{\varepsilon\alpha_2}, \psi^* = \psi e^{\varepsilon\alpha_3} \\ \theta^* = \theta e^{\varepsilon\alpha_4}, \phi^* = \phi e^{\varepsilon\alpha_5} \end{array}\right\} \quad (15)$$

By putting equation (15) into equation (11) – (13) yield's the following which transformed coordinates $(x, y, \psi, \theta, \phi)$ to $(x^*, y^*, \psi^*, \theta^*, \phi^*)$, where$\varepsilon$is parameter of the group and $\alpha$is the real number.

$$\varepsilon(2\alpha_2 + \alpha_1 - 2\alpha_3)(1 + \lambda)\left[\frac{\partial\psi}{\partial y}\frac{\partial^2\psi}{\partial x\partial y} - \frac{\partial\psi}{\partial x}\frac{\partial^2\psi}{\partial y^2}\right] + \\ \beta e^{\varepsilon(2\alpha_1 + 3\alpha_2 - 3\alpha_3)}\left[\left(\frac{\partial\psi}{\partial y}\right)^2\frac{\partial^3\psi}{\partial x^2\partial y} + \left(\frac{\partial\psi}{\partial x}\right)^2\frac{\partial^3\psi}{\partial y^3} - 2\frac{\partial\psi}{\partial y}\frac{\partial\psi}{\partial x}\frac{\partial^3\psi}{\partial x\partial y^2}\right] \\ = e^{\varepsilon(3\alpha_2 - \alpha_3)}\frac{\partial^3\psi}{\partial y^3} + e^{-\varepsilon\alpha_4}[(1 + \lambda)Ra\theta] - \\ e^{-\varepsilon\alpha_5}[(1 + \lambda)RaN_r\phi] - (1 + \lambda)M^2\left[e^{\varepsilon(\alpha_2 - \alpha_3)}\frac{\partial\psi}{\partial y} - e^{\varepsilon(\alpha_1 + 2\alpha_2 - 2\alpha_3)}\right] \\ -e^{\varepsilon(\alpha_2 - \alpha_3)}(1 + \lambda)\frac{1}{K}\frac{\partial\psi}{\partial y} \quad (16)$$

$$e^{\varepsilon(\alpha_1 + \alpha_2 - \alpha_3 - \alpha_4)}Pr\left[\frac{\partial\psi}{\partial y}\frac{\partial\theta}{\partial x} - \frac{\partial\psi}{\partial x}\frac{\partial\theta}{\partial y}\right] = \\ e^{\varepsilon(2\alpha_2 - 4\alpha_4)}\left[1 + \frac{4}{3}N(Ct - \theta)^3\right]\frac{\partial^2\theta}{\partial y^2} + e^{\varepsilon(2\alpha_2 - 4\alpha_4)}4N[Ct + \theta]^2\left(\frac{\partial\theta}{\partial y}\right)^2 \\ +e^{\varepsilon(-\alpha_4)}Q\theta + e^{\varepsilon(2\alpha_2 - \alpha_4 - \alpha_5)}N_b\frac{\partial\phi}{\partial y}\frac{\partial\theta}{\partial y} \\ +e^{\varepsilon(2\alpha_2 - 2\alpha_4)}N_t\left(\frac{\partial\theta}{\partial y}\right)^2 \quad (17)$$

$$e^{\varepsilon(\alpha_1 + \alpha_2 - \alpha_3 - \alpha_5)}Le\left[\frac{\partial\psi}{\partial y}\frac{\partial\phi}{\partial x} - \frac{\partial\psi}{\partial x}\frac{\partial\phi}{\partial y}\right] = e^{\varepsilon(2\alpha_2 - \alpha_5)}\frac{\partial^2\phi}{\partial y^2} \\ +e^{\varepsilon(2\alpha_2 - \alpha_4)}\frac{N_t Sr}{N_b}\frac{\partial^2\theta}{\partial y^2} - e^{-\varepsilon(\alpha_5)}\gamma\phi \quad (18)$$

By comparing various exponential terms of equations (16) - (18) the invariant of the system is achieved as obtained below

$$\left.\begin{array}{l} \left.\begin{array}{l} 2\alpha_2 + \alpha_1 - 2\alpha_3 = 2\alpha_1 + 3\alpha_2 - 3\alpha_3 \\ = 3\alpha_2 - \alpha_3 = -\alpha_4 = -\alpha_5 = \alpha_2 - \alpha_3 = \\ \alpha_1 + 2\alpha_2 - 2\alpha_3 = \alpha_2 - \alpha_3 \end{array}\right\} \\ \left.\begin{array}{l} \alpha_1 + \alpha_2 - \alpha_3 - \alpha_4 = 2\alpha_2 - 4\alpha_4 = \\ 2\alpha_2 - 4\alpha_4 = -\alpha_4 = 2\alpha_2 - \alpha_4 - \alpha_5 \\ = 2\alpha_2 - 2\alpha_4 \end{array}\right\} \\ \left.\begin{array}{l} \alpha_1 + \alpha_2 - \alpha_3 - \alpha_5 = 2\alpha_2 - \alpha_5 \\ = 2\alpha_2 - \alpha_4 = -\alpha_5 \end{array}\right\} \end{array}\right\} \quad (19)$$

From equation (14) the invariance of the boundary conditions becomes

$$\alpha_1 = \alpha_3, \qquad \alpha_2 = \alpha_4 = \alpha_5 = 0 \quad (20)$$

Subject to the solutions of equation (19) using equation (20) the groups of transformations (15) take the form:

$$\Gamma: \left.\begin{array}{l} x^* = xe^{\varepsilon\alpha_1}, y^* = y, \psi^* = \psi e^{\varepsilon\alpha_1}, \\ \theta^* = \theta, \phi^* = \phi \end{array}\right\} \quad (21)$$

Also, employing Taylor series expansions yields

$$\left.\begin{array}{l} x^* - x = \varepsilon x\alpha_1 + 0(\varepsilon^2), \\ y^* - y = 0, \\ \psi^* - \psi = \varepsilon\psi\alpha_1 + 0(\varepsilon^2), \\ \theta^* - \theta = 0, \\ \phi^* - \phi = 0 \end{array}\right\} \quad (22)$$

Since$\alpha_1 \neq 0$, rewrite equation (22) to give the following characteristic equations

$$\left.\begin{array}{l} \frac{x^* - x}{x\alpha_1} = \varepsilon, y^* - y = 0, \frac{\psi^* - \psi}{\psi\alpha_1} = \varepsilon, \\ \theta^* - \theta = 0, \phi^* - \phi = 0 \end{array}\right\} \quad (23)$$

Now, in terms of differentials equation (23) becomes

$$\frac{d\psi*}{\alpha_1\psi^*} = \frac{dx^*}{x^*\alpha_1} \quad (24)$$

$$dy^* = d\theta^* = d\phi^* = 0 \quad (25)$$

By integrating equation (24) – (25) the following similarity transformations were determined:

$$\left.\begin{array}{l} y^* = \eta, \psi^* = x^* f(\eta), \theta^* = \theta(\eta), \\ \phi^* = \phi(\eta) \end{array}\right\} \quad (26)$$

Where η is a variable and$f(\eta)$, $\theta(\eta)$, and $\phi(\eta)$ are functions Employing equation (26) into equations (11) – (14), the equations below emerged:

$$f''' + (1 + \lambda)[ff'' - f'^2] - \beta[f^2 f''' - 2f'ff''] - \\ (1 + \lambda)\left[M(f' - \beta ff'') + \frac{1}{K}f'\right] + \\ (1 + \lambda)Ra[\theta - N_r\phi] = 0 \quad (27)$$

$$\left[1 + \frac{4}{3}N(Ct + \theta)^3\right]\theta'' + 4N[Ct + \theta]^2\theta'^2 + \\ Pr[f\theta' + Q\theta + N_b\phi'\theta' + N_t\theta'^2] = 0 \quad (28)$$

$$\phi'' + \frac{N_t Sr}{N_b}\theta'' + Le[f\phi' - \gamma\phi] = 0 \quad (29)$$

While the boundary conditions read:

$$\left.\begin{array}{l}\left.\begin{array}{l} f=S, f'=1, \\ \theta'=-B_i(1-\theta), \\ \phi=1 \end{array}\right\} at\eta=0 \\ f'\to 0, \theta\to 0, \phi\to 0\} as\eta\to\infty \end{array}\right\} \quad (30)$$

Physical Quantities

The interested physical term are the reduced Skin friction coefficients(C_f), the reduced Nusselt number(Nu) and reduced Sherwood number(Sh)

$$C_f=\frac{1}{2}Re_x^{-\frac{1}{2}}C_f=f''(0) \quad (31)$$

$$Nu=Re_x^{-\frac{1}{2}}Nu=-\theta'(0) \quad (32)$$

$$Sh=Re_x^{-\frac{1}{2}}Sh=-\phi'(0) \quad (33)$$

Computational Method

The nonlinear boundary-value problem was solved using MATLAB bvp4c with a relative tolerance of 10^{-10}, while the solver automatically adapted the computational mesh to satisfy the prescribed error tolerance. The systems of coupled nonlinear differential equations placed in equations (27) – (29) were scaled down into first order initial value problem via the following transformation:

$$(h_1,h_2,h_3,h_4,h_5,h_6,h_7,h_8,h_9,h_{10})=(f,f',f'',f''',\theta,\theta',\theta'',\phi,\phi',\phi'') \quad (34)$$

$$\begin{pmatrix} h_1\\ h_2\\ h_3\\ h_4\\ h_5\\ h_6\\ h_7 \end{pmatrix}=\begin{pmatrix} y_2\\ y_3\\ \left[\frac{1}{1-\beta y_1^2}\right]\left[-2\beta y_2y_1y_3-(1+\lambda)[y_1y_3-y_2^2]+(1+\lambda)\left[M(y_2-\beta y_1y_3)+\frac{1}{K}y_2\right]+(1+\lambda)Ra[y_4-Nry_6]\right]\\ y_5\\ \frac{1}{\left[1+\frac{4}{3}N(C_t+y_4)^3\right]}\left[-4N(Ct+y_4)^2y_5^2-Pr(y_1y_5+Qy_4+Nby_7y_5+Nty_5^2)\right]\\ y_7\\ -\frac{NtSr}{Nb}y_5'-Le[y_1y_7-\gamma y_6] \end{pmatrix}$$

Result Validation

To ensure the authenticity of the existent result, in the absence of the Jeffrey parameter and porosity parameter, the present work coincides with that of Hayat *et al*. (2010), Turkyilmazoglu (2013), and Ahmad *et al*. (2022). From table (3.1), which illustrates numerous values for magnetic parameter(M), our result with Ahmad *et al*. (2022) established a brilliant agreement. So, it defends the use of the numerical code for the present work. Also, table (3.2) and figure (2) show the numerical results and graphical results, respectively, when $Ra\neq 0$ for both present results and Ahmad *et al*. (2022). From figure 3, shows that nonlinear thermal radiation emits more heat than linear thermal radiation.

Table 2: Comparative Numerical Outcomes for the Reduced Skin Friction $f''(0)$ when $\beta=Ra=S=Bi=\lambda=0$ and $K\to\infty$ with Previous Work

M	Hayat *et al.* (2010)	Turkyilm Azoglu (2013)	Ahmad *et al.* (2022)	Present Results
0.0	-1.000000	- 1.000000	-1.000000	-1.000000
0.5	-1.224747	-1.224744	-1.224745	-1.224745
1.0	-1.414217	-1.414213	-1.414215	-1.414214

Table 3: Comparative Analysis of the Reduced Skin-Friction Coefficient for the Linear Thermal Radiation Model of Ahmad et al. (2022) and the Present Nonlinear Thermal Radiation Model

M	Ahmad et al. (2022) Linear thermal Radiation	Present Resu;ts Nonlinear thermal radiation
0.0	-1.178175524	-2.320956912
0.5	-1.404724611	-2.504852607
1.0	-1.621708085	- 2.676532794

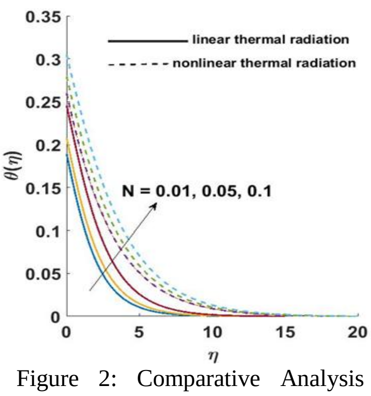

Figure 2: Comparative Analysis Between Linear Thermal Radiation and Nonlinear Thermal Radiation for $\theta(\eta)$Outlines

RESULTS AND DISCUSSION

This exact fragment is allotted to scrutinize the soret effect of stable-state magnetohydrodynamic heat transfer of Jeffrey nanofluid with nonlinear thermal radiation. In this study, the default values are: $Nr = \frac{1}{2}$, $N = \frac{1}{100}$, $S = \frac{1}{10}$, $Ra = \frac{1}{100}$, $Le = \frac{1}{5}$, $M = \frac{1}{5}$, $Nt = \frac{1}{5}$, $\gamma = \frac{1}{10}$, $Pr = \frac{71}{100}$, $\lambda = \frac{1}{2}$, $Nb = \frac{1}{5}$, $K = \frac{1}{2}$, $\beta = \frac{1}{5}$, $Ct = \frac{1}{5}$, $Q = \frac{1}{100}$, $Bi = \frac{1}{10}$, $Sr = \frac{1}{10}$. Unless otherwise detail.

Velocity Outline

However, figure (3 - 6) illustrates the effect of velocity outline for different values of Rayleigh number, porosity parameter, Jeffrey parameter, and magnetic parameter respectively. By enhancing the values of Rayleigh number, the velocity of Jeffrey nanofluid goes up and the opposite direction is noticed for raising porosity, Jeffrey and magnetic parameters. Physically, when Rayleigh number is less than zero the flow is unstable and turbulence can occur. The porosity parameter provides accommodations for outflows of heat through the exterior. As a result, the inter molecular forces that are holding the molecules of the Jeffrey nanofluid will become stronger. An increase in Jeffrey parameter signifies weaker retardation time. The reduction in the velocity profile with increasing Jeffrey parameter is physically consistent with the viscoelastic behaviour reported in previous Jeffrey-fluid investigations. Generally, magnetic parameters yield Lorentz forces; such forces cause a resistance in the flow of the fluid. This behaviour agrees with the general MHD trends reported in earlier studies.

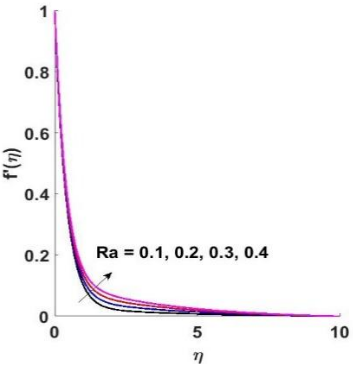

Figure 3: $f'(\eta)$ Outlines for Ra

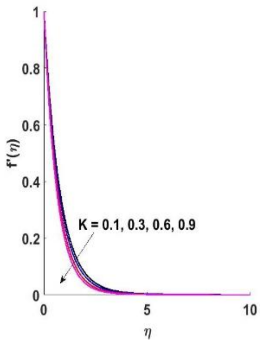

Figure 4: $f'(\eta)$ Outlines for K

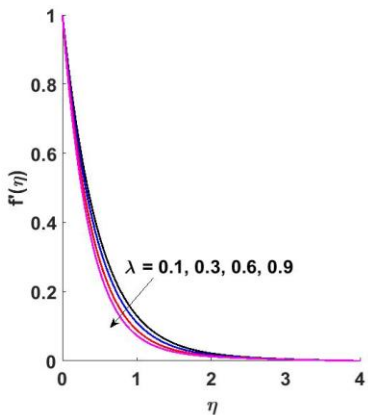

Figure 5: $f'(\eta)$ Outlines for λ

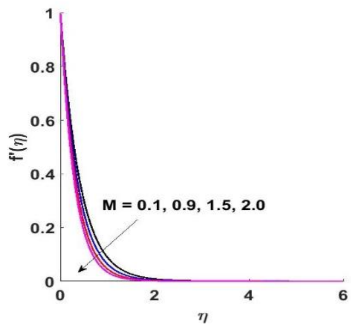

Figure 6: $f'(\eta)$ Outlines for M

Temperature Outline

In addition, figure (7 - 9) showcases the outcome of nonlinear thermal radiation**,** heat source-sink parameter and Biot number on temperature contour. An increase in nonlinear thermal radiation, heat source-sink parameter and Biot number leads to the increase in temperature outline. Generally, more heat is produced by raising nonlinear thermal radiation. The enhancement of the temperature field with increasing nonlinear thermal radiation parameter agrees with the findings reported in the literature on radiative nanofluid transport. The heat transfer occurrence is improved by the presence of an external heating source. Biot number signifies the quotient of conductive resistance in solids to the connective resistance in thermal boundary layer.

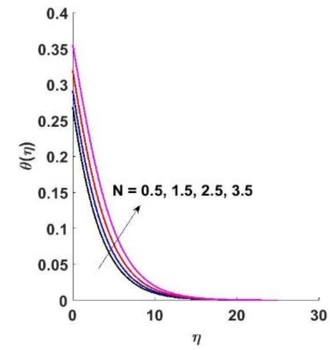

Figure 7: $\theta(\eta)$ Outlines for N

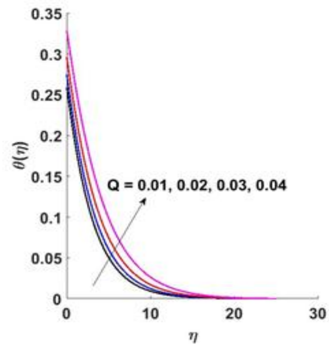

Figure 8: $\theta(\eta)$ Outlines for Q

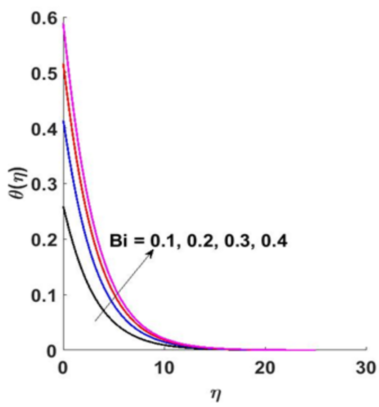

Figure 9: $\theta(\eta)$ Outlines for Bi

Concentration Outline

Furthermore, figures (10 – 12) depicts the upshots of concentration contour for diverse values of Lewis number, chemical reaction parameter and Soret parameter respectively. The concentration contour goes down by raising the values of Lewis number, chemical reaction parameter and took the reverse case for Soret parameter. Actually, the Lewis number is a quotient of thermal diffusivity to mass diffusivity. Thus, the boundary layer thickness will rise if the fluid viscosity is more than the diffusion coefficient. Soret is a thermal gradient which is used for solute transportation. Physically, increase in Soret brings about higher thermal gradient which raises the convective flow. The present results further indicate that the Soret mechanism remains important when coupled with Jeffrey fluid behaviour, magnetic effects, porous resistance, and nonlinear thermal radiation, thereby extending the physical interpretation of the thermo-diffusion effects reported in earlier studies.

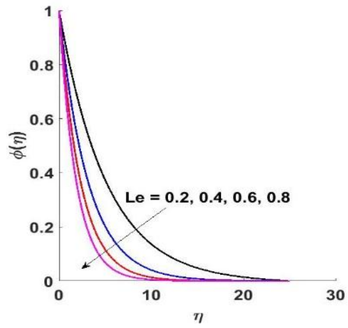

Figure 10: $\phi(\eta)$ Outlines for Le

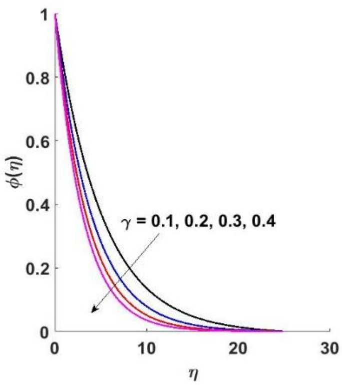

Figure 11: $\phi(\eta)$ Outlines for γ

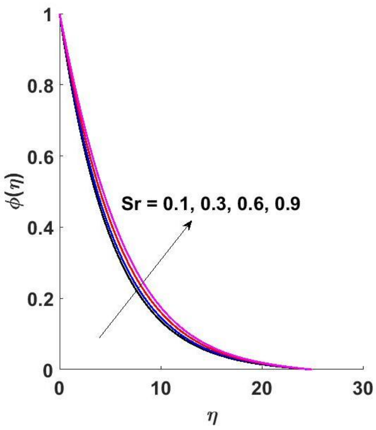

Figure 12: $\phi(\eta)$ Outlines for Sr

Also, the influence of the Jeffrey parameter and magnetic parameter on skin friction is disclosed in figure (13) and (14) respectively. By boosting the Jeffrey parameter and magnetic parameter the skin friction is diminished. Generally, the nanofluids are slightly depressed as the Jeffrey parameter is increased. Also, the use of magnetic parameter yields Lorentz force, this force causes a resistance in the Jeffrey nanofluid flow which decreases the thickness of the momentum boundary layer.

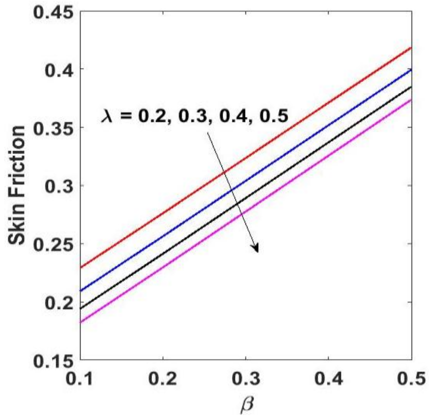

Figure 13: Skin Friction Outlines for λ

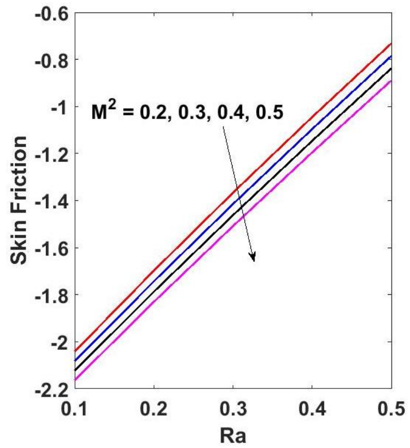

Figure 14: Skin Friction Outlines for M

Also, the effect of Brownian motion and Biot number on Nusselt number is noticed in figure (15) and (16) respectively. By strengthening Brownian motion and Biot number the Nusselt number goes down. This reduction is due to the nanoparticles of high thermal conductivity which is driven away from the hot sheet to the quiescent fluid.

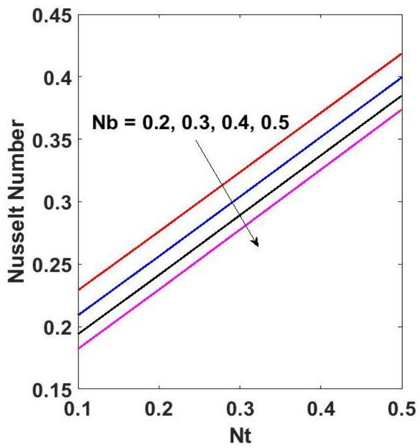

Figure15: Nusselt Number Outlines for Nb

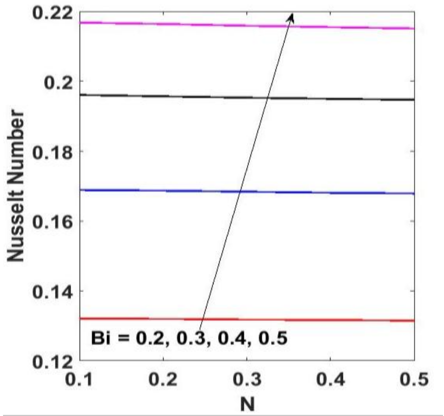

Figure 16: Nusselt Number Outlines forBi

Furthermore, the effect of Brownian motion and Soret parameter on Sherwood number is noticed in figure (17) and (18) respectively. The Sherwood number goes up by enhancing Brownian motion and Soret parameter.

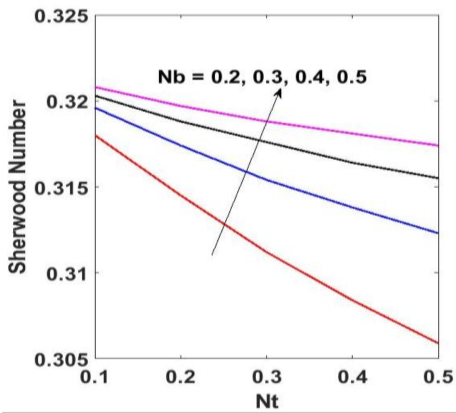

Figure 17: Sherwood Number Outlines forNb

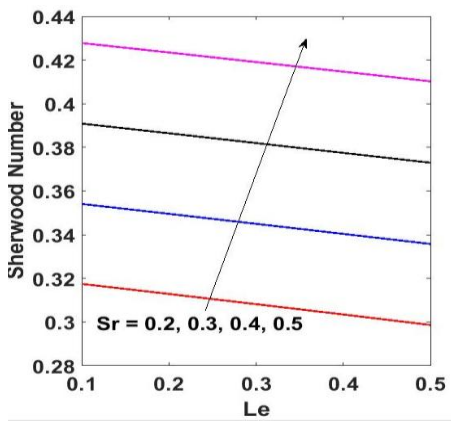

Figure 18: Sherwood Number Outlines forSr

CONCLUSION

The numerical exploration of the stable state magnetohydrodynamic heat transfer of Jeffrey nanofluid laminar boundary flow of a perpendicular plate influenced by viscous dissipation was carried out. The Lie group approach was used to alter the main partial differential equations into ordinary differential equations solved numerically. Some of the significant findings are:

i. The strength of the porosity, magnetic, and Jeffrey parameters slows down the velocity of the Jeffrey nanofluid.
ii. By boosting the thermal radiation parameter, the heat source-sink parameter, and the Biot number, escalates the flow of temperature.
iii. By escalating the chemical reaction, the Lewis number diminished the concentration of the Jeffrey nanofluid and went up with the Soret parameter.
iv. Skin friction is diminished by enhancing the Jeffrey parameter and the magnetic parameter.
v. By raising Brownian motion, it reduces the Nusselt number and takes the reverse case for the Biot number.
vi. The Sherwood number goes up by enhancing Brownian motion and the Soret parameter.

vii. Model validation against the published results demonstrated excellent agreement, with a maximum relative discrepancy of approximately 0.00021% in the reduced skin-friction values.

Limitations

Despite the comprehensive consideration of the coupled transport mechanisms, the present study has certain limitations. The analysis is restricted to steady-state flow in a stretching sheet geometry, with the thermophysical properties and modelling assumptions maintained throughout the computational domain. In addition, the study considers the specific fluid model and parameter ranges adopted in the present formulation. Consequently, the obtained results may not fully represent flow configurations involving transient effects, alternative geometries, or substantially different fluid and material properties.

Future Work

Future investigations may extend the present framework to unsteady MHD flow and alternative geometries, including stretching surfaces, porous channels, and curved configurations. Further studies could also examine different nanoparticle shapes and hybrid or ternary nanofluids to determine their influence on heat and mass transport. Other potentially important extensions include variable thermophysical properties, Forchheimer porous resistance, viscous dissipation, Joule heating, and non-Fourier heat-conduction models. Such extensions would provide a broader understanding of coupled momentum, heat, and mass transfer in MHD non-Newtonian flows and enhance the applicability of the present model to practical thermal and engineering systems.

REFERENCES

Abbas, Z., Hussain, S., Rafiq, M. Y., & Hasnain, J. (2020). Oscillatory slip flow of Fe3O4 and Al2O3 nanoparticles in a vertical porous channel using Darcy's law with thermal radiation. *Heat Transfer*, *49*(6), 3228-3245.

Abbasi, F. M., Shehzad, S. A., Hayat, T., & Alhuthali, M. S. (2016). Mixed convection flow of Jeffrey nanofluid with thermal radiation and double stratification. *Journal of Hydrodynamics, Ser. B*, *28*(5), 840-849.

Abdullahi, B., Isah, B. Y., Ibrahim, Y. S., & Murtala, M. H. (2022). Upshot of Slip Velocity and Thermal Radiation on Magnetohydrodynamic Transient Fluid Flow through Vertical Walls. *Int J Theor Appl Math*, *8*(3), 65-77.

Ahmad, B., Nawaz, A., Smida, K., Khan, S. U., Khan, M. I., Abbas, T., ... & Galal, A. M. (2022). Thermal diffusion of Maxwell nanoparticles with diverse flow features: Lie group simulations. *International Communications in Heat and Mass Transfer*, *136*, 106164.

Ali, B., Jubair, S., Aluraikan, A., Abd El-Rahman, M., Eldin, S. M., & Khalifa, H. A. E. W. (2023). Numerical investigation of heat source induced thermal slip effect on trihybrid nanofluid flow over a stretching surface. *Results in Engineering*, *20*, 101536.

Aman, S., Khan, I., Ismail, Z., Salleh, M. Z., Alshomrani, A. S., & Alghamdi, M. S. (2017). Magnetic field effect on Poiseuille flow and heat transfer of carbon nanotubes along a vertical channel filled with Casson fluid. *AIP Advances*, *7*(1).

Aman, S., Khan, I., Ismail, Z., Salleh, M. Z., & Tlili, I. (2018). A new Caputo time fractional model for heat transfer enhancement of water based graphene nanofluid: An application to solar energy. *Results in physics*, *9*, 1352-1362.

Bafakeeh, O. T., Ahmad, B., Noor, S., Abbas, T., Khan, S. U., Khan, M. I., ... & Guedri, K. (2022). Nonlinear thermal diffusion and radiative stagnation point flow of nanofluid with viscous dissipation and slip constrains: Keller box framework applications to micromachines. *Micromachines*, *13*(11), 1839.

Bidemi, O. F., & Ahamed, M. S. (2019). Soret and Dufour effects on unsteady Casson magneto-nanofluid flow over an inclined plate embedded in a porous medium. *World Journal of Engineering*, *16*(2), 260-274.

Das, K., Sarkar, A., & Kundu, P. K. (2017). Nanofluid flow over a stretching surface in presence of chemical reaction and thermal radiation: an application of Lie group transformation. *Журнал Сибирского федерального университета. Серия «Математика и физика»*, *10*(2), 146-157.

Disu, A. B., Michael, W., Ishola, C. Y., & Ajibola, S. O. (2025). Numerical investigation of magnetohydrodynamic Jeffrey fluid flow with nonlinear thermal radiation in a vertical channel. *Power Eng. Eng. Thermophys*, *4*(4), 241-252.

Disu, A. B., Michael, W., Salawu, S. O., Ishola, C. Y., & Oyelami, O. A. (2026). Analysis of MHD Poiseuille and Couette flow of an engine oil-based hybridized nanomaterial in an inclined device. *Next Research*, 101987.

Hasnain, J., & Abid, N. (2023). Numerical investigation for thermal growth in water and engine oil-based ternary nanofluid using three different shaped nanoparticles over a linear and nonlinear stretching sheet. *Numerical Heat Transfer, Part A: Applications*, *83*(12), 1365-1376.

Hayat, T., Mustafa, M., & Pop, I. (2010). Heat and mass transfer for Soret and Dufour's effect on mixed convection boundary layer flow over a stretching vertical surface in a porous medium filled with a viscoelastic fluid. *Communications in Nonlinear Science and Numerical Simulation*, *15*(5), 1183-1196.

Hayat, T., Qayyum, S., & Alsaedi, A. (2017). Mechanisms of nonlinear convective flow of Jeffrey nanofluid due to nonlinear radially stretching sheet with convective conditions and magnetic field. *Results in physics*, *7*, 2341-2351.

Irfan, M., & Muhammad, T. (2024). Computational framework of MHD radiative heat transfer to Carreau nanofluid with Soret-Dufour effects and activation energy. *ZAMM-Journal of Applied Mathematics and Mechanics/Zeitschrift für Angewandte Mathematik und Mechanik*, *104*(3), e202300410.

Isah, B. Y., Abdullahi, B., & Seini, I. Y. (2022). On transient MHD heat transfer within a radiative porous channel due to convective boundary conditions. *Heat Transfer*, *51*(6), 5140-5158.

Ishtiaq, B., Nadeem, S., & Alzabut, J. (2023). Effects of variable magnetic field and partial slips on the dynamics of

Sutterby nanofluid due to biaxially exponential and nonlinear stretchable sheets. *Heliyon*, *9*(7).

Jha, B. K., & Samaila, G. (2023). Nonlinear approximation for buoyancy-driven mixed convection heat and mass transfer flow over an inclined porous plate with Joule heating, nonlinear thermal radiation, viscous dissipation, and thermophoresis effects. *Numerical Heat Transfer, Part B: Fundamentals*, *83*(4), 139-161.

Kandasamy, R., Loganathan, P., & Arasu, P. P. (2011). Scaling group transformation for MHD boundary-layer flow of a nanofluid past a vertical stretching surface in the presence of suction/injection. *Nuclear Engineering and Design*, *241*(6), 2053-2059.

Khan, S. U., & Shehzad, S. A. (2020). Flow of Jeffrey nanofluids over convectively heated oscillatory moving sheet with magnetic field and porosity effects. *Journal of Porous Media*, *23*(9).

Khan, M. I., Waqas, M., Hayat, T., Alsaedi, A., & Khan, M. I. (2017). Significance of nonlinear radiation in mixed convection flow of magneto Walter-B nanoliquid. *International Journal of Hydrogen Energy*, *42*(42), 26408-26416.

Lawal, M. O., Kasali, K. B., Ogunseye, H. A., Oni, M. O., Tijani, Y. O., & Lawal, Y. T. (2022). On the mathematical model of Eyring–Powell nanofluid flow with non-linear radiation, variable thermal conductivity and viscosity. *Partial Differential Equations in Applied Mathematics*, *5*, 100318.

Michael, W., & Isah, B. Y. (2023). On a conducting Jeffrey nanofluid flow over a stretching sheet with porous material and diffusion-thermo: a Lie group approach. *Journal of Nanosciences Research & Reports*, *5*(2), 1-9.

Michael, W., Isah, B. Y., Aminu, M., & Ahmed, A. (2023). Analyzing steady state heat and mass transfer in Jeffrey nano fluid with nonlinear thermal radiation. *Int J Theor Appl Math*, *9*(3), 23-34.

Muhammad, T., Waqas, H., Manzoor, U., Farooq, U., & Rizvi, Z. F. (2022). On doubly stratified bioconvective transport of Jeffrey nanofluid with gyrotactic motile microorganisms. *Alexandria Engineering Journal*, *61*(2), 1571-1583.

Nasir, S., Berrouk, A. S., Gul, T., & Ali, A. (2023). Develop the artificial neural network approach to predict thermal transport analysis of nanofluid inside a porous enclosure. *Scientific Reports*, *13*(1), 21039.

Rana, G. C. (2021). Effects of rotation on Jeffrey nanofluid flow saturated by a porous medium. *Journal of Applied Mathematics and Computational Mechanics*, *20*(3), 17-29.

Rashidi, M. M., Momoniat, E., Ferdows, M., & Basiriparsa, A. (2014). Lie group solution for free convective flow of a nanofluid past a chemically reacting horizontal plate in a porous media. *Mathematical Problems in Engineering*, *2014*(1), 239082.

Reddy, M. G., & Makinde, O. D. (2016). Magnetohydrodynamic peristaltic transport of Jeffrey nanofluid in an asymmetric channel. *Journal of Molecular Liquids*, *223*, 1242-1248.

Shuaibu, A., Bello, Y., Kallamu, A. M., Ojemeri, G., & Abdulrauf, R. (2026). Thermal radiation and suction/injection effects on mixed convection heat transfer in a porous coaxial cylindrical channel. *FUDMA Journal of Sciences*, *10*(4), 45-52.

Sobamowo, M. G. (2018). Combined effects of thermal radiation and nanoparticles on free convection flow and heat transfer of casson fluid over a vertical plate. *International Journal of Chemical Engineering*, *2018*(1), 7305973.

Turkyilmazoglu, M. (2013). The analytical solution of mixed convection heat transfer and fluid flow of a MHD viscoelastic fluid over a permeable stretching surface. *International Journal of Mechanical Sciences*, *77*, 263-268.

Waqas, M., Shehzad, S. A., Hayat, T., Khan, M. I., & Alsaedi, A. (2019). Simulation of magnetohydrodynamics and radiative heat transport in convectively heated stratified flow of Jeffrey nanofluid. *Journal of Physics and Chemistry of Solids*, *133*, 45-51.

Williams, M., & Yabo, I. B. (2024). The upshots of Dufour and Soret in stretching porous flow of convective Maxwell nanofluid with nonlinear thermal emission. *International Journal of Theoretical and Applied Mathematics*, *10*(3), 38-50.

Yabo, I. B., Williams, M., Mustafa, A., & Ahamd, A. (2023). The upshot of nonlinear thermal emission on a conducting Jeffrey nanofluid flow over a stretching sheet: a Lie group approach. *Saudi Journal of Civil Engineering*, *7*(8), 178-191.

Zin, N. A. M., Khan, I., Shafie, S., & Alshomrani, A. S. (2017). Analysis of heat transfer for unsteady MHD free convection flow of rotating Jeffrey nanofluid saturated in a porous medium. *Results in physics*, *7*, 288-309.